MAGNETIC RESONANCE IN MEDICINE

Carbon-13 "Magic-Angle" Sample-Spinning Nuclear Magnetic Resonance Studies of Human Myelin, and Model Membrane Systems

Cynthia Husted, Bernard Montez, Carl Le, Mario A. Moscarello, Eric Oldfield

We have obtained high-field (11.7 Tesla), high-resolution carbon-13 solid-state "magic-angle" sample-spinning nuclear magnetic resonance (NMR) spectra of a variety of phospholipids, sphingolipids, myelin and white matter samples, resolving and assigning over 40 resonances in the spectra of human and bovine myelin. The NMR results indicated no large spectral changes due to sample preparation, sample freezing, or brain location, and also no changes in myelin structure detectable via light microscopy, electron microscopy, thin layer chromatography, or sodium dodecyl sulfate-polyacrylamide gel electrophoresis, attributable to the sometimes lengthy NMR data acquisition process. Human myelin and white matter chemical shift assignments were made based on ^{13}C "magic angle" sample spinning (MAS) NMR spectra of individual model lipids, as well as on spectra of lipid mixtures. In all myelin samples there were essentially no features attributable to membrane proteins, with the exception of one small feature due to Cζ of Arg residues, primarily in the myelin basic proteins. The general similarity between the model lipid and intact myelin spectra suggested no major effects of protein on lipid mobility. We have also investigated human myelin samples as a function of developmental age (4, 15, 48 months and adult), and our results showed only small changes in overall lipid composition, although there were significant decreases in lipid hydrocarbon chain unsaturation with age, as determined by computer line-shape simulations of myelin and model compounds. The spectrum of an infant leukoencephalopathy myelin showed marked decreases in galactocerebrosides. Overall, the ability to resolve and assign over 40 resonances in the ^{13}C MAS NMR spectra of myelin, and to detect changes as a function of development and disease, should provide a useful starting point for further more detailed studies of myelin membrane molecular motions, and function.

Key words: NMR; myelin; membranes.

INTRODUCTION

Model and biological membranes have been studied with NMR spectroscopy for over 25 years, with the ultimate goal of resolving individual carbon, proton (and deuteron) resonances, in order to investigate lipid composition, structure, function, and dynamics. The early ^{1}H, ^{2}H, and ^{13}C NMR studies, although successful in providing considerable basic insight into the static and dynamic properties of membranes, were usually characterized by either broad lines and low resolution, required ultrasonication (which has the potential of disrupting the membrane's native structure), or required difficult, time-consuming and costly isotopic substitution (1–6). Previous researchers have reported ^{1}H solution NMR spectra of lyophilized bovine myelin (7), ^{1}H wide-line and "high-resolution" NMR spectra of sonicated and unsonicated bovine myelin (8), ^{13}C NMR spectra of sonicated myelin (9), as well as ^{13}C NMR spectra of sonicated peripheral nerve endoneurium (the connective tissue sheath which surrounds nerve fibers within a fasciculus) (10), but few myelin membrane resonances were resolved in each case. More recently, we have reported high-resolution ^{1}H and ^{13}C "magic-angle" sample spinning (MAS) NMR spectra of unsonicated model membranes, and myelin, which eliminate many of the these drawbacks, and give well resolved spectra of both model membranes and intact myelin (11–13). Unlike the situation with sonicated model or myelin membranes, both lipid and sterol resonances can be resolved with use of the ^{13}C MAS NMR technique (9, 14).

"Magic-angle" sample spinning averages out the second rank tensor interactions that usually govern ^{13}C NMR line widths in the solid state. The ability to obtain high-resolution ^{13}C NMR spectra of unsonicated systems is especially important in biological samples such as myelin, which, due to its large water content, and complexity, is much less suitable for ^{1}H analyses. The dominant line-broadening mechanisms for ^{13}C in unsonicated systems are the ^{13}C chemical shift anisotropy (CSA) and heteronuclear (^{13}C-^{1}H) dipolar coupling. Homonuclear dipolar interactions for ^{13}C nuclei are minimal, due to its low natural abundance. Biological membranes generally exist in a fluid liquid crystalline state, in which the lipids exhibit a considerable degree of motional freedom. These motions—lateral diffusion within the plane of the bilayer, axial rotation, and fatty acid *gauche-trans* isomerization—effectively reduce the dipolar coupling and CSA of the lipid systems. Thus, the residual CSA can be easily averaged at relatively low spinning speeds of ~1.5 to 3.0 kHz, and heteronuclear dipolar broadening can generally be removed by use of moderate decoupling power. However, in order to have good spectral resolution, very high fields are needed for systems as complex as myelin, spectra obtained at 8.45 T (data not shown) being noticeably less well resolved.

Myelin is a particularly attractive candidate for ^{13}C

MRM 29:168–178 (1993)

From the Department of Chemistry, University of Illinois at Urbana-Champaign, Urbana, Illinois (C.H., B.M., C.L., E.O.); and the Department of Biochemistry, Hospital for Sick Children, University of Toronto, Toronto, Ontario, Canada (M.A.M.)

Address correspondence to: Eric Oldfield, Ph.D., Department of Chemistry, University of Illinois at Urbana Champaign, 505 South Matthews Avenue, Urbana, IL 61801.

Received November 25, 1991; revised May 13, 1992; accepted May 13, 1992.

This work was supported by the United States Public Health Service (National Institutes of Health grant GM-40426).

0740-3194/93 $3.00

MAS NMR investigation, due to its very high lipid content, which is about 70:30 lipid:protein (by weight) compared to e.g., about 30:70 for mitochondrial and many other biomembranes. The lipid weight percentages for human central nervous system (CNS) myelin frequently referred to are (15): cholesterol (CHOL), 27.7%; galactocerebroside (GC), 22.7%; phosphatidalethanolamine (PE plasmalogen, PEpl), 12.3%; phosphatidylcholine (PC), 11.2%; sphingomyelin (SM), 7.9%; phosphatidylserine (PS), 4.8%; sulfatide, 3.8%; phosphatidylethanolamine (PE), 3.3%; and phosphatidylinositol (PI), 0.6%. Although no one lipid is specific to myelin, these percentages indicate that it is unusually enriched in cholesterol, galactocerebrosides and PE plasmalogen, relative to other biomembranes. The most abundant fatty acids found in human brain white matter (WM) are palmitic [16:0], stearic [18:0], nervonic [24:1], oleic [18:1], and arachidonic [20:4]. Sastry (16) gives an extensive summary of the previously reported myelin lipid fatty acid compositions.

In this article we report recent results aimed at assigning each of the myelin resonances, as well as presenting initial results on myelin lipid compositional changes with development, by using the ^{13}C MAS NMR technique. Without use of ultrasonication or isotopic labeling, we can resolve and assign over 40 resonances, due to the phospholipids, sphingolipids, and cholesterol that make up the lipid component of intact myelin membranes. These results present the most highly resolved spectra obtained to date on an intact biological membrane, and represent a "benchmark" with which to make comparisons with other myelins, for example from different species (E. Oldfield, J. Haase, T. Bowers, J. Patterson, C. Husted, B. Montez, L. Moran, A. L. de Vries, M. A. Moscarello, to be published), as well as for investigating the topic of lipid-protein interactions in model membrane systems (J. Patterson, T. Bowers, B. Montez, X. Sham, C. Le, M. A. Moscarello, E. Oldfield, to be published).

EXPERIMENTAL

NMR Spectroscopy

All ^{13}C NMR spectra were obtained on a "home-built" NMR spectrometer, which operates at 500 MHz for ^{1}H, and consists of an Oxford Instruments (Osney Mead, U.K.) 2.0-inch bore, 11.7 Tesla superconducting solenoid, together with a Nicolet (Madison, WI) Model 1280 computer system, a Henry Radio (Los Angeles, CA) Model 1002 radiofrequency amplifier, an Amplifier Research (Souderton, PA) Model 200L radiofrequency amplifier, and either a 5-mm Doty Scientific (Columbia, SC) MAS NMR probe or a 5-mm multinuclear solution NMR probe (Cryomagnet Systems, Indianapolis, IN). For ^{13}C MAS NMR experiments, dipolar decoupled Bloch decays were recorded using 8.5 to 9.0 μs 90° pulse widths, spinning rates of ca. 3.0 kHz, and CYCLOPS phase cycling (19). Spectra were acquired in double precision mode, due to the large dynamic range, and files were block-averaged in order to monitor possible sample changes with time. Temperatures were adjusted via a gas flow cryostat, and the values reported were monitored with a Doric (San Diego, CA) Trendicator, the thermocouple being placed near the sample. All ^{13}C MAS NMR spectra were referenced with respect to an external standard of adamantane [δ = 39.5, 28.5 ppm from TMS], using the convention that high frequency, low field, paramagnetic or deshielded values are denoted as positive (IUPAC δ-scale).

Electron Microscopy

Samples for electron microscopy were fixed with 1% osmium tetroxide, dehydrated using an ascending series of ethanol concentrations, embedded in epoxy resin, and the resulting sections stained with 20% uranyl nitrate. Electron micrographs were obtained on a Hitachi (Tarrytown, NY) Model H-600 transmission electron microscope, operating at 75 kV.

Sample Preparation

Egg yolk SM, bovine brain α-hydroxygalactocerebroside (HGC), bovine brain non-GC, and 1,2-dipalmitoyl-*sn*-glycero-3-phosphocholine (dipalmitoylphosphatidylcholine, DPPC), were obtained from Sigma Chemical Company (St. Louis, MO). Bovine brain sulfatides, containing a mixture of α-hydroxy and nonhydroxy fatty acids, were obtained from Supelco (Bellefonte, PA). Bovine brain PE-plasmalogen, (PEpl), egg yolk PE, PS, and bovine PI were from Avanti Polar Lipids, Inc. (Birmingham, AL). PI and PS were also obtained from Lipid Products (South Nutfield, Surrey, U.K.). All phospholipids and sphingolipids were used without further purification. If the lipids came in solution, the solvent was first removed by means of flowing N_2, then the last traces of solvent were removed by lyophilizing overnight. Lipid samples were prepared for NMR spectroscopy by addition of 50 wt% $^{2}H_2O$ (Sigma). Cholesterol was from Aldrich (Milwaukee, WI), and was recrystallized three times from ethanol, before use. Sample purity was monitored periodically, via thin-layer chromatography, on Eastman Chromagram silica-gel plates (No. 6061; Eastman Kodak, Rochester, NY), by using a $CHCl_3$:MeOH:7 *M* NH_4OH (230:90:15, v/v/v) solvent system, with molybdenum blue as a visualizing agent (20).

Human myelin and white matter samples were obtained at The Hospital for Sick Children in Toronto, and from Dr. W. W. Tourtellotte, of the National Neurological Research Bank. All samples were received frozen, and formalin free. Human white matter was centrifuged in glass distilled water at 45,000 × *g* overnight. Human myelin was isolated from autopsy samples by use of a sucrose gradient, as described elsewhere (21). Bovine white matter was obtained fresh from Allens Farm (Homer, IL).

Quantitative thin layer chromatography of myelin lipids was performed on silica gel 60 F_{254} 20 × 20 cm plates (E. Merck, Darmstadt, Germany), which were activated at 90°C for 30 min prior to use, and developed in chloroform: methanol:water (14:6:1, v/v/v). Samples of WM, or myelin, were solubilized in chloroform:methanol (2:1, v/v) to a final concentration of 10 mg/ml. A 30-μl aliquot of each sample was spotted, and the plate developed

until the solvent front reached the top. Lipids were visualized by charring with 50% H_2SO_4 at 90°C for 10 min. Charred plates were scanned with an LKB (Piscataway, NJ) Ultroscan XL enhanced laser densitometer. Sodium dodecyl sulfate-polyacrylamide gel electrophoresis was carried out according to the method of Laemmli (22), by using an LKB Pharmacia electrophoresis system, and the gels scanned with the same densitometer noted above.

RESULTS AND DISCUSSION

Myelin Spectra: General Aspects

Figure 1 shows the complete ^{13}C MAS NMR spectrum of a sample of normal adult human myelin. There are about 40 quite well resolved peaks, although we indicate below that there are up to 65 peaks and shoulders, since this helps with an accounting of all expected resonances. In some cases, e.g., Cβ of PE, $C^{3,4}$ of GC, and many aliphatic carbons, sites that are not resolvable in a Bloch decay spectrum can actually be resolved by use of a cross-polarization (CP) spectral editing method (data not shown). All myelin and WM spectra shown in this publication are proton decoupled Bloch decays, since cross polarization generally results in complex signal intensity behavior, due at least in part to the wide range of molecular motions present. Not only do optimum mix times vary from <1 msec to >30 msec, but for the more "liquid-like" resonances, there are complex intensity oscillations, possibly due to J-cross polarization and off-resonance effects. Thus, we find that the simple proton-decoupled Bloch decay gives the most readily interpretable results.

An initial inspection of Fig. 1 suggests that there are three fairly distinct regions in myelin and (white matter) spectra: In the high field region, of 10 to 45 ppm, most of the saturated and quaternary carbons of cholesterol, and the fatty acyl chains can be identified (peaks 39–65, see below), in sharp contrast to the results seen with sonicated myelin (9), where the cholesterol features are greatly broadened, due to slow vesicle rotation (11, 14). In the region of ~45 to 85 ppm (peaks 17–38), are primarily the more polar sp^3 carbons from the head group and backbone carbons of the phospholipids, sphingolipids, and galactolipids, together with several cholesterol methine ring carbons. Finally, in the low field region (peaks 1–15), are the unsaturated carbons, together with (see below) Cζ of Arg, and the galactose anomeric

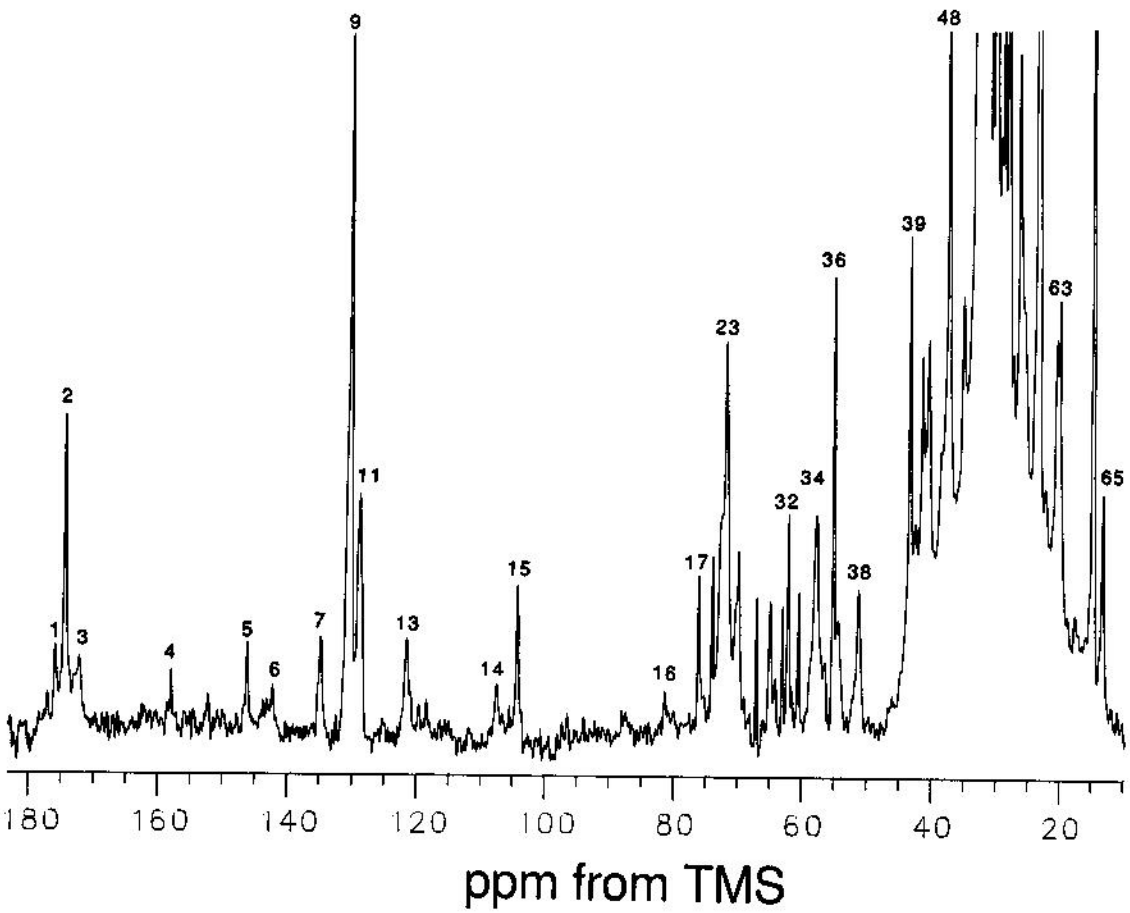

FIG. 1. 125.7 MHz (11.7 Tesla) proton-decoupled ^{13}C Fourier transform MAS NMR spectrum of normal (non-neurological death, 43-year-old male, died of myocardial infarction) human myelin at 37°C, 3.0 kHz MAS, recorded using 90° rf pulse excitation, 16,452 acquisitions, 8-k points in the time domain, 5-s recycle time, 26,314 Hz spectral width, and 10 Hz line broadening due to exponential multiplication. About 45 to 50 peaks can usually be identified in human adult myelin; additional weak shoulders or very small peaks are also included (see e.g., Table 1) for a total of 65 features, since this helps with "book-keeping" all of the resonances expected, based on known chemical composition. Some peaks having bad spectral overlaps can also be resolved by using CP spectral-editing.

carbons. As expected based on results with membrane proteins in general, few resonances attributable to protein are seen, due to their rigid nature (large chemical shift anisotropy), overall complexity (broad spectral dispersion), and the possibility of incomplete decoupling due to motional rates on the order of the ^1H decoupling field strength (in Hz).

A likely exception to this statement is the resonance observed at 157.8 ppm, (peak 4) which we believe is due primarily to arginine Cζ residues of the myelin basic proteins (MBP), a protein family which contains ~11% arginine, the molecular weight of the most abundant MBP being ~18.5 kDa.

We tested this assignment in two ways. First, we have shown previously (23) that Arg-Cζ resonances undergo a ~0.20 ppm upfield shift when the adjacent protons are exchanged with ^2H, to give the [$^2H_6$]isotopomer:

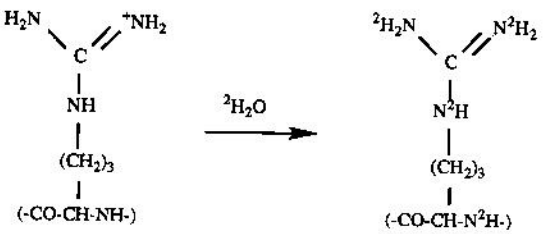

We thus exchanged two myelin samples with ^2H_2O three times, and we obtained a ~0.2 ppm upfield shift for peak 4 (only) upon deuteration (results not shown). When the samples were reequilibrated with ^1H_2O, the chemical shift of peak 4 returned to 157.8 ppm, consistent with an assignment to Cζ of Arg. In addition, peak 4 was absent in myelin lipid extracts, supporting a protein origin. Another possibility was that this feature could arise from Cδ of creatine, a possible metabolic impurity. However, since the relative intensity of peak 4 was constant—i.e., it could not be washed out, and did not vary from sample to sample, this possibility seemed unlikely.

A second approach to the assignment of this resonance was to make a quantitative estimate of the amount of Cζ represented by peak 4, and to compare this with the known Arg-Cζ contents of the myelin proteins. Using known lipid and protein compositions we deduced that if peak 4 arises from MBP Arg-Cζ it should represent ≈0.13% of the total ^{13}C NMR integrated intensity. Experimentally, we found ≈0.16%, close to the value expected for observation of all Arg-Cζ resonance in MBP. A similar calculation for the proteolipid protein (24), which has seven possible surface arginines, yields a contribution of ≈0.07, for a total of 0.20% for Arg-Cζ.

We now wish to discuss several important topics that relate to any analysis of myelin NMR spectra. In particular, we must consider whether there may be differences between myelin spectra, due either to myelin preparation, sample freezing, brain location, or data acquisition.

The ^{13}C MAS NMR spectra of myelin and intact WM from brain, as well as 'intact' spinal cord, were all essentially indistinguishable (25). WM, in addition to containing myelin, includes axons, oligodendroglia, and astrocytes. However, the concentration of axonal, glial and

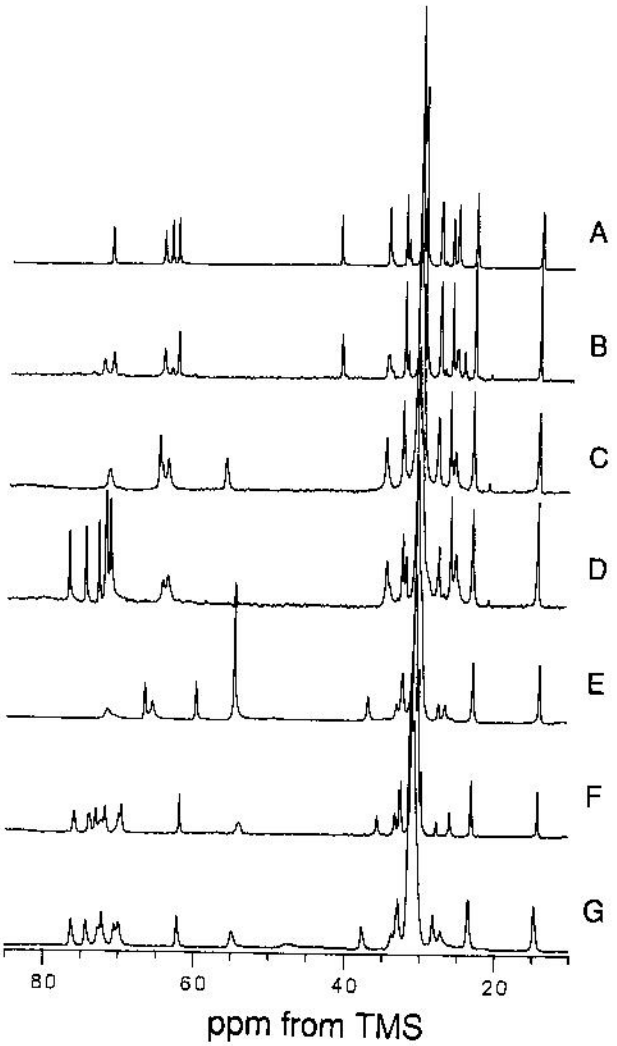

FIG. 2. 125.7 MHz (11.7 Tesla) proton-decoupled ^{13}C MAS NMR spectra of liquid crystalline phase phospholipids, and sphingolipids, in excess water. (A) Egg PE, 75°C, 6000 acquisitions; (B) bovine brain PE plasmalogen, 37°C, 5000 acquisitions; (C) bovine brain phosphatidylserine, 45°C, 6000 acquisitions; (D) bovine liver phosphatidylinositol, 21°C, 3000 acquisitions; (E) bovine brain sphingomyelin, 60°C, 2000 acquisitions; (F) bovine brain α-hydroxygalactocerebrosides, 80°C, 2000 acquisitions; (G) bovine brain nonhydroxy galactocerebrosides, 80°C, 2000 acquisitions. Recycle times were 5 s and spectra were subject to 5 Hz linebroadening due to exponential multiplication. The MAS rates were all ≈3.0 kHz.

astrocyte membrane lipids in WM is so low that they should be virtually undetectable. WM was centrifuged overnight in glass distilled water, which resulted in removal of the soluble species previously reported (26). Thus, the similarity between WM and myelin suggests that the sucrose density gradient used to prepare myelin caused no major perturbations—at least as viewed by ^{13}C MAS NMR.

We have also investigated the effects of sample freezing, since all human samples were obtained as frozen tissue. Due to the difficulty of obtaining fresh, formalin-free human brain tissue, fresh bovine brain WM was used. There were no differences between the fresh and

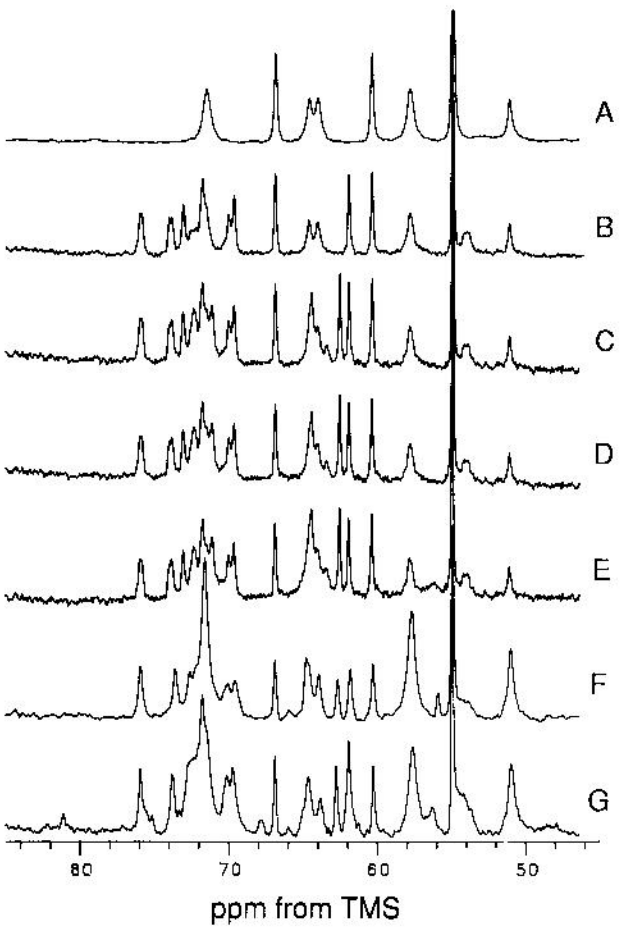

FIG. 3. 125.7 MHz (11.7 Tesla) proton-decoupled ^{13}C MAS NMR "spectra" of myelin lipids, obtained by digital addition of individual lipid spectra, together with experimental spectra of a myelin lipid mixture and an adult human myelin, in the headgroup/backbone carbon spectral region. (A) 1:1 mole ratio cholesterol/egg yolk lecithin (EYL), 50 wt% D_2O, 21°C; (B) EYL/CHOL + bovine brain galactocerebroside (GC); (C) EYL/CHOL + GC + PE plasmalogen (PEpl); (D) EYL/CHOL + GC + PEpl + sphingomyelin (SM); (E) EYL/CHOL + GC + PEpl + SM + phosphatidylserine + phosphatidylinositol; (F) lipid mixture containing all expected lipids in correct proportions for myelin membrane; (G) Normal adult human myelin, 37°C. Since CHOL does not disperse in water, we used a 1:1 mole ratio PC/CHOL in (A) then added digitally appropriate contributions of other pure lipid spectra, based on known myelin compositions. The spectrum in (F) is the *experimental* result for a complete lipid mixture.

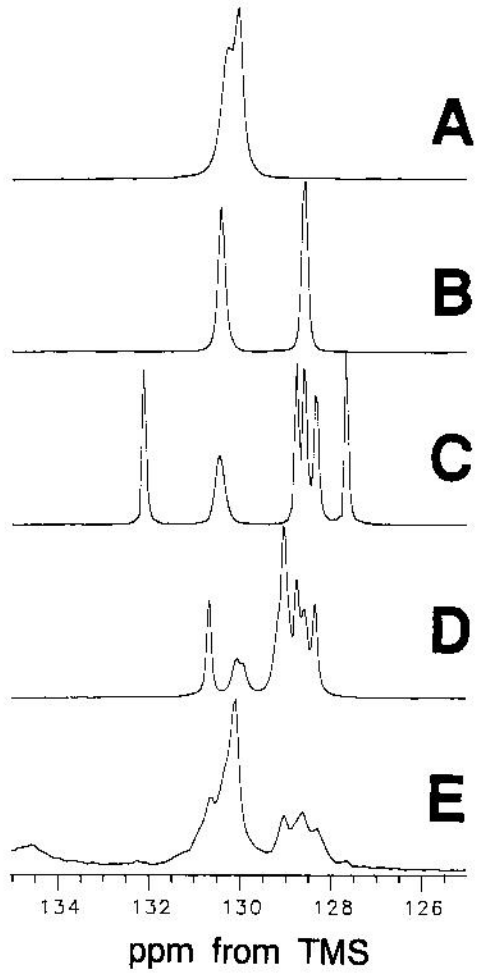

FIG. 4. 125.7 MHz (11.7 Tesla) proton-decoupled ^{13}C MAS NMR spectra in the olefinic carbon region of: (A) di-oleoyl PC, [18:1]; (B) di-linoleoyl PC, [18:2]; (C) di-linolenoyl PC, [18:3]; (D) di-arachidonoyl PC, [20:4]; (E) normal adult human myelin, 37°C. Spectral conditions all basically as for Fig. 1.

frozen (for 1 month) WM and myelin spectra, except a somewhat lower signal-to-noise ratio in the fresh WM spectra, because the sample was not hard-pelleted (25). Bovine WM was also used to assess spectral variability due to sample (brain) location. WM was isolated from the following brain regions: corpus callosum; frontal lobes; occipital lobes; midbrain and brainstem. Differences between myelin spectra in each of these five different brain regions were quite small, given the uncertainties associated with achievable signal-to-noise ratios (25).

A final concern was that there could be sample changes due to some unspecified "degradation" during the typically ~12 h required for data acquisition. We thus conducted several checks of myelin integrity in order to arrive at what we believe are acceptable myelin data acquisition conditions.

First, we obtained microtome tissue preparations on myelin and WM samples before and after NMR data acquisition, by using Weil's method, a regressive myelin staining technique using hematoxylin and ferric alum (27). Stained bands of myelin could clearly be seen in all samples (25). Second, transmission electron micrographs were obtained of myelin samples before and after NMR data acquisition. These micrographs showed the presence of compact myelin (25), but would not indicate small chemical changes. Consequently, thin layer chromatography (TLC) and sodium dodecyl sulfate-polyacrylamide gel electrophoresis (SDS-PAGE) analyses were performed, and the results again showed no detectable changes in lipid or protein structure after NMR data acquisition (25). Sample pH was also monitored before and after NMR data acquisition, by using a microelectrode which inserts into the NMR rotor. The pH remained constant, having a value of 6.9 ± 0.2.

Spectra were also acquired in batches of 3000 scans, for

a total of 10 batches, in order to monitor any possible spectral changes due to myelin breakdown. Initial results showed a noticeable linebroadening after ~24 h. We initially thought this might be due to lipid oxidation, and thus spun our samples using dry N_2. However, the spectra then broadened even more quickly, and the sample mass was observed to decrease, due to dehydration. When the dehydrated sample was rehydrated, the NMR spectrum returned to normal, thus confirming that the major spectral change was due to sample dehydration, rather than lipid oxidation. We thus routinely used tight "o"-ring and Teflon-tape-sealed Macor rotors and moist air as our drive gas. Under these conditions we observe essentially no mass (H_2O) loss during data acquisition, and no spectral changes.

Finally, time-batched spectra of multiple portions of a single myelin preparation were obtained, in order to try to detect more subtle effects which might be occurring on a time scale less than that required for a single-batch experiment. For example, ^{13}C MAS NMR spectra of four portions of the same myelin preparation were acquired in four time series, of: 0 to 5, 5 to 10, 10 to 15, and 15 to 20 h, resulting in 16 spectra. The spectra at the same time intervals (e.g., four spectra at 5–10 h) were then averaged in order to obtain four high signal-to-noise ratio myelin spectra, one for each time increment (0–5, 5–10, 10–15, and 15–20 h). When using tightly sealed rotors, these spectra showed no changes with time (25). While we cannot definitively state that there might not be spectral changes in, say, the first 30 min, when viewed in light of all of the other control experiments, this possibility seems remote.

Thus, the control experiments show no detectable sample changes with time, as evidenced by visible microscopy (Weil's method), transmission electron microscopy, TLC, SDS-PAGE, pH or time-batched NMR measurements. If spectral changes do occur on the <5-h time scale, they are not detectable using the analytical methods listed above, and the bovine myelin results are very similar to those obtained on fresh WM.

Spectral Assignments

We have assigned most of the ^{13}C MAS NMR features in human myelin, shown in Fig. 1, based upon peak intensity and chemical shift information. The chemical shifts of the individual lipids were assigned based upon solution assignments in the literature, as well as some additional 2D assignments made in this laboratory (25). In addition, the ^{13}C MAS NMR spectra of the individual lipid components were used to "build-up" a "synthetic" myelin spectrum, which was in quite good accord with that observed, further substantiating the assignments given. We thus discuss first, briefly, the assignments of the major individual lipids (Fig. 2), followed by a discussion of the build-up of the myelin spectrum using individual lipids, and a synthetic myelin lipid mixture (Fig. 3), followed by a consideration of the question of lipid unsaturation (Figs. 4 and 5).

Figure 2 shows the ^{13}C MAS NMR spectra of the following model compounds (as 50 wt% dispersions in ^2H_2O): A, Egg PE; B, PEpl; C, PS; D, PI; E, SM; F, HGC; G,

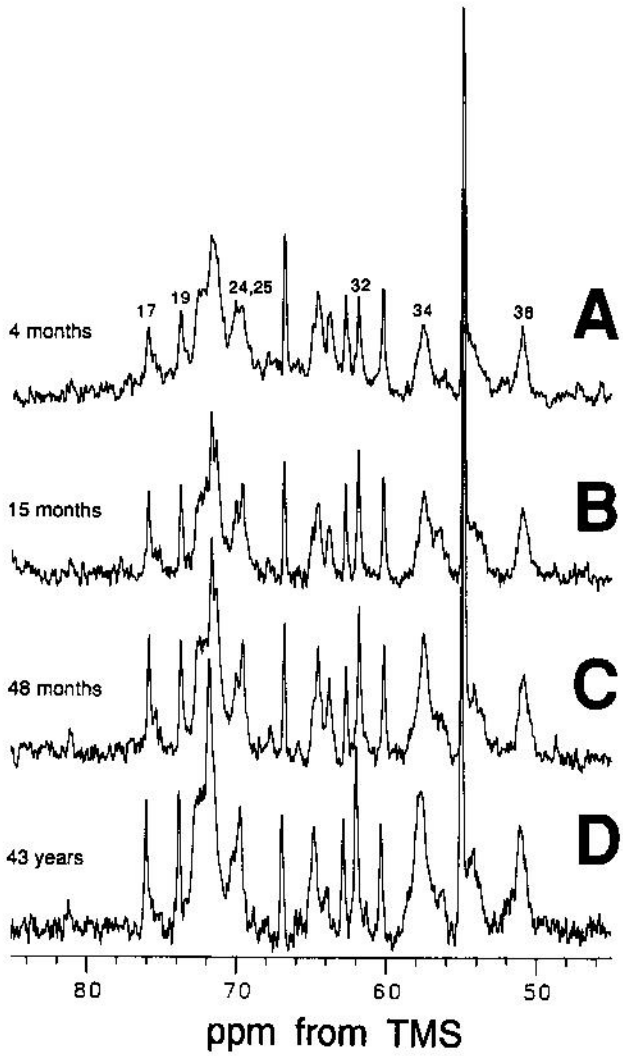

FIG. 5. 125.7 MHz (11.7 Tesla) ^{13}C MAS NMR spectra in the headgroup/backbone carbon region of human myelin, as a function of developmental age. (A) 4-month infant; (B) 15-month infant; (C) 48-month infant; (D) normal adult (43 years, male, died from myocardial infarction). Spectral conditions basically as in Fig. 1.

GC. The ^{13}C MAS NMR chemical shifts of these model lipids are incorporated into the myelin assignments given in Table 1. More details are available in Ref. 25. Figure 2B shows the headgroup and saturated hydrocarbon chain region of PE plasmalogen, a phospholipid formed from dihydroxyacetone phosphate and a long chain alcohol, resulting in an α,β-unsaturated vinyl ether instead of a fatty acid in the *sn*-1 position of the glycerol. Plasmalogen, which comprises most of the PE, is the most abundant phospholipid in myelin. ^{13}C MAS NMR assignments of PE plasmalogen were based on those of Murari *et al.* (28), and results for the lipid-water dispersion are given in Table 1. A small impurity resonance remains unassigned, at 63.6 ppm. TLC results rule out PE (diester) contamination. Phase heterogeneity cannot be ruled out, neither can the formation of lyso-PE.

Figures 2C-G show the ^{13}C MAS NMR spectra of several other model phospholipids and sphingolipids, most of which are significant components of myelin. We have

Table 1
Human Myelin, White Matter, and Model Compound ^{13}C MAS NMR Chemical Shift Assignments[a]

Feature No.[a]	Myelin δ (ppm)	WM δ (ppm)	Assignment	Model (δ, ppm)
1	175.9	175.8	SM, GC-C1″	174.9,[b] 176.7[c]
2	174.3	174.4	acyl C1 (C═O)	174.3[d]
3	172.4	172.2	PS-Cγ	172.0[e]
4	157.8	157.9	arginine-Cζ	157.8[f]
5	146.2	146.1	PEpl-C1′	145.8[g]
6	142.2	142.6	cholesterol-C5	142.6[d]
7	134.7	135.0	SM, GC-C4′	134.8,[b] 135.0[c]
8	130.6	130.7	[18:1]-C10[h]; [24:1]-C16; [18:2]-C9, C13; [20:4]-C15	130.3,[i] 130.4,[j] 130.6[k]
9	130.0	130.2	[18:1]-C9[h]; [24:1]-C15; [20:4]-C5; SM, GC-C5′ sulfatides-C4′,5″	130.0,[i,k] 129.9,[k] 130.9,[b] 130.3,[c] 130.1[i]
10	129.0	129.1	[20:4]-C9, C11, C12	129.0[k]
11	128.6	128.7	[18:2]-C10, C12; [20:4]-C6, C8	128.6,[i,k] 128.7[k]
12	128.3	128.4	[20:4]-C14	128.3[k]
13	121.3	121.7	cholesterol-C6	121.0[d]
14	107.5	107.4	PEpl-C2′	107.2[g]
15	104.1	104.2	sugar-C1	104.1[c]
16	81.0	81.0	sulfatides-sugar C3	81.0[j]
17	76.0	76.1	sugar-C5	76.0[c]
18	75.0	75.5	PI	76.9[m]
19	73.8	73.9	sugar-C3	73.0[c]
20	73.3	73.5	PI	74.8[m]
21	72.4	72.8	SM, GC-C2″ (α-OH); PEpl-C2; PI-C3″	71.8,[b] 73.1,[c] 72.5,[g] 73.0[m]
22	72.2	72.3	GC-C3′; PI-C4″, C6″	72.4,[c] 72.1[m]
23	71.8	71.9	glycerol-C2; cholesterol-C3; SM-C3′; PI-C2″; PEpl-C3; sugar C2; sulfatides-C3′	71.6,[d] 71.8[b,c] 71.5,[m] 71.3,[g] 71.8,[l]
24	70.1	70.1	GC-C1′	70.0[c]
25	69.8	69.8	sugar-C4	69.7[c]
26	66.8	67.0	PC, SM-Cβ	66.7,[b] 67.2[d]
27	66.0	66.2	SM-C1′	66.0[b]
28	65.0	65.1	C3: PC, PI, PS, PE; PEpl-Cα; PS-Cβ	64.5,[d,g] 64.6,[e,m,n] 64.5[g]
29	64.7	64.8	C3: PC, PI, PS, PE; PEpl-Cα; PS-Cβ	64.5,[d,g] 64.6,[e,m,n] 64.5[g]
30	63.9	64.0	C1: PC, PI, PS, PE	64.0,[d] 63.9,[m] 63.6[e,n]
31	62.8	62.9	PE-Cα; PEpl-C1	62.7[g,n]
32	62.0	62.0	sugar-C6	61.9[c]
33	60.3	60.4	PC, SM-Cα	60.2,[d] 59.9[b]

[a] A number of features occur as very weak shoulders, but occur frequently, and some are resolved in CP edited spectra. Most assignments (except that for Arg-Cζ) are based on ^{13}C MAS NMR chemical shifts, which in turn are referenced to literature solution values (25).
[b] Shifts given for liquid crystalline bovine SM at 60°C (37).
[c] Shift for liquid crystalline bovine α-OH galactocerebroside at 80°C (38, 39).
[d] Shift given for DPPC/CHOL at 21°C (12).
[e] Shift for liquid crystalline bovine PS at 21°C (40).
[f] Solution shift for Cζ of arginine in hen egg white lysozyme, 21°C (23).
[g] Shift for liquid crystalline bovine brain PE plasmalogen, at 37°C (28).
[h] Acyl chain given is most likely type; longer chains with same amount of unsaturation would give essentially the same shift. [18:1], [24:1], and [26:1] are expected, and C9 (15) cannot be differentiated in myelin from C10 (16).

based our ^{13}C MAS NMR peak assignments of human myelin (and WM) on the model systems described above, and our myelin assignments are given in Table 1.

The highly resolved nature of the ^{13}C MAS NMR spectra of myelin also enabled us to observe many cholesterol resonances, as well as those of the lipid headgroups, backbones, and fatty acid (or alcohol) sidechains. In order to help confirm these assignments, we have carried out a "computer modeling" of the myelin spectrum shown in Fig. 1 by adding together, digitally, spectra of the various individual lipids. The resulting spectra are shown in Figs. 3A–E.

Figure 3A shows the ^{13}C MAS NMR spectrum of the head group/backbone region (~50–80 ppm) of a 1:1 (mole ratio) mixture of egg lecithin and cholesterol. Most of these features can be readily detected in the intact myelin spectrum, Fig. 5G. Addition of GC resulted in the addition of a number of additional peaks due to the sugar lipid (Fig. 3B). With addition of PE, PEpl, SM, PS, and PI, Fig. 3E, we obtained quite good agreement with all of the major spectral features in the myelin spectrum, Fig. 3G. The obvious exception is that the cholesterol resonance intensities are low, due to our starting with an experimental 50 mole% PC/CHOL mixture, Fig. 3A. (A maximum of 50 mole% cholesterol can incorporate into the lipid bilayer.) However, additional results on a lipid mixture (Fig. 3F) containing the expected CHOL levels (for myelin) are in general agreement with the myelin result (Fig. 3G), although there are some intensity differences, which may be attributable to protein.

Fatty acyl chain ^{13}C NMR resonance assignments of the model phospholipids and myelin were based on those of Batchelor *et al.* (29) and Sillerud *et al.* (30), and on the ^{13}C MAS NMR spectra and simulations of L-α-dioleoyl PC

Table 1 *Continued*

Feature No.[a]	Myelin δ (ppm)	WM δ (ppm)	Assignment	Model (δ ppm)
34	57.6	57.8	cholesterol-C14, C17	57.7[d]
35	56.2	56.3	PS-Cα	55.5[e]
36	54.9	55.0	PC, SM-Cγ; SM-C2'; sulfatides-C2'	54.8,[b] 55.1[d] 55.2[l]
37	54.2	54.1	GC-C2'	53.9[c]
38	50.9	51.1	cholesterol-C9	51.2[d]
39	43.2	43.3	cholesterol-C13	43.4[d]
40	42.4	42.6	cholesterol-C4	42.5[d]
41	41.3	41.4	PE-Cβ	41.1[n]
42	40.8	41.0	cholesterol-C12	41.1[d]
43	40.8	40.8	PEpl-Cβ	40.9[g]
44	40.4	40.4	cholesterol-C24	40.2[d]
45	38.3	38.4	cholesterol-C1	38.5[d]
46	37.3	37.4	cholesterol-C10, C20, C22	37.5,[d] 37.3[d]
47	34.9	35.1	acyl-C2; SM, GC-C3"; sulfatides-C6'	35.0,[d] 36.9,[b] 35.6,[c] 34.9[l]
48	32.6	32.6	chain C(ω-2); cholesterol-C7, C8; SM, GC-C6', C2" (non-OH)	32.7,[d,o] 33.1[b]
49	31.6	31.7	$(CH_2)n$[p]; cholesterol-C2[q]	31.4[d]
50	31.0	31.2	$(CH_2)n$[p]	31.4[d]
51	30.7	30.7	$(CH_2)n$[p]	31.4[d]
52	30.4	30.4	$(CH_2)n$[p]	31.4[d]
53	30.0	30.0	$(CH_2)n$[p]	31.4[d]
54	29.2	29.2	cholesterol-C16	29.1[d]
55	28.7	28.8	cholesterol-C25	28.5[d]
56	27.9	27.9	[18:1]-C8, C11[h]; [18:2]-C8, C14; [20:4]-C16	27.9,[i] 28.0,[i] 27.8[k]
57	27.2	27.4	[20:4]-C4	27.2[k]
58	26.2	26.3	[18:2]-C11; [20:4]-C7, C10, C13	26.3[j,k]
59	25.6	25.6	cholesterol-C15, C23; acyl-C3	25.6[d]
60	23.1	23.2	cholesterol-C26, C27; chain C(ω-1)	22.9,[d] 23.2[d]
61	q	22.2	cholesterol-C11	22.1[d]
62	20.4	20.4	cholesterol-C19	20.2[d]
63	19.8	19.9	cholesterol-C21	19.9[d]
64	14.6	14.6	chain C(ω)	14.2[d]
65	13.0	13.1	cholesterol-C18	13.1[d]

[i] Shift for di-oleoyl PC at 26°C.
[j] Shift for di-linoleoyl PC at 26°C.
[k] Shift for di-arachidonoyl PC at 26°C. The eight $\Delta^{5,8,11,14}$ Z,Z,Z,Z carbons cannot be specifically resolved and assigned in any lipid-water system. The general pattern of increased shielding in the following sequence: 15,5,6,8,12,9,11,14 is likely, based on studies of other lipids, and linewidth considerations (41).
[l] Shift for bovine brain sulfatide/DMPC, 80°C (38).
[m] Shift for liquid crystalline wheat germ PI, at 21°C (42, 43).
[n] Shift for liquid crystalline egg PE, at 75°C (12, 28).
[o] Shift for liquid crystalline bovine brain non-hydroxygalactocerebrosides, 80°C (38, 39).
[p] Cannot be specifically assigned, due to peak overlaps.
[q] Resonance obscured.

[18:1], L-α-dilinoleoyl PC [18:2], L-α-dilinolenoyl PC [18:3], and L-α-diarachidonoyl PC [20:4], shown in Fig. 4. As can be seen from Fig. 4, our results indicated high levels of 18:1/24:1 and 20:4 fatty acids in human myelin, but very small levels of linoleic (18:2) or linolenic (18:3), consistent with expectation (16). In the high-field region of the spectrum (10–40 ppm), extensive spectral overlaps with saturated chain and the numerous sterol carbon atom resonances occur, making assignments in this region more complex.

In order to better understand the features in the olefinic carbon region of myelin, Fig. 4E, which are of importance for studies of myelin development, we have carried out computer simulations of model and myelin fatty acid alkene regions. Spectral simulations of the Δ^9 18:1 and $\Delta^{5,8,11,14}$ 20:4 lecithins were in good agreement with theoretical intensities (data not shown, see Ref. 25 for details). We then used the 18:1 and 20:4 spectral simulation parameters as input data to simulate the major features of the olefinic region of the myelin spectrum. Under the simplifying assumption that only the monoenoic and polyenoic (20:4) fatty acids contribute to intensity in the ~128 to 131 ppm region, which we believe to be a good assumption based on previous work (31, 32), myelin olefinic spectral simulation results were in good agreement with the experimental spectra.

If we let the mole fraction of 20:4 be X, then the polyunsaturate content can be obtained from any given spectrum by a simple integration of the upfield, 128 to 129 ppm region ("B" = polyunsaturate) and the downfield, 129 to 131 ppm region ("A" = monounsaturate), since:

$$\frac{B}{A} = \frac{6X}{2X + 2(1 - X)}; X(\%) = 33.33\ B/A \qquad [1]$$

Thus, an estimate of the polyunsaturate/monounsaturate region can be readily determined from an experimental spectrum—a point we discuss below in more detail, since this ratio changes with myelin development. Based on ^{13}C MAS NMR simulations of 11 normal

adult human myelins, we find a polyunsaturate/mono unsaturate ratio of 0.17 ± 0.04. Solid-state NMR does not currently have the resolution of other techniques for fatty acid analysis, e.g., capillary gas chromatography-mass spectrometry. Nevertheless, we believe such simulations give a good account of the polyenoic (primarily 20:4) to monoenoic (primarily 18:1, 24:1) fatty acid compositions. Our results are consistent with reported results (31, 32), and perhaps more importantly, they open up the possibilities of studies of chain dynamics as a function of development.

Infant and Abnormal Myelins

The results presented above all pertain to adult human myelins, but the topic of the changes that occur in myelin as a function of development is in itself of some interest. The most extensive studies of lipid composition as a function of development have been those of Svennerholm and Vanier (31) and Svennerholm *et al.* (32). These workers found that the amounts of cholesterol and galactolipid increased slightly up to 2 years, whole choline phosphoglycerides decreased somewhat. For most phospholipids, the proportion of saturated and polyunsaturated fatty acids decreased, while mono-unsaturated fatty acids increased.

Figure 5 shows the ^{13}C MAS NMR spectra in the head group/backbone carbon region of human myelin samples from 4; 15; and 48-month-old infants, and a 43-year-old normal adult. Although the changes in the head group/backbone carbon region are not large, there appear to be small increases in cholesterol (peaks No. 34, 38) and galactocerebroside (peaks No. 17, 19, 24, 25, 32) peak intensities with increasing age, a result consistent with that reported by Svennerholm et al. (32). Using the phospholipids as an "internal standard," Svennerholm et al. found a ≈10 to 15% increase in cholesterol and galactolipids from ~4 months to ≈70 years, the largest changes occurring in the first ~5 to 10 years. Such changes, however, are about the same as the errors associated with any quantitative ^{13}C NMR analysis of a system as complex as myelin, and indeed, even the analytical results (32) are quite scattered.

Far more impressive changes as a function of development are exhibited in the *olefinic* region of the ^{13}C MAS NMR spectra of human myelin, as shown in Figures 6A-D. Here, we show the region 126 to 133 ppm down-

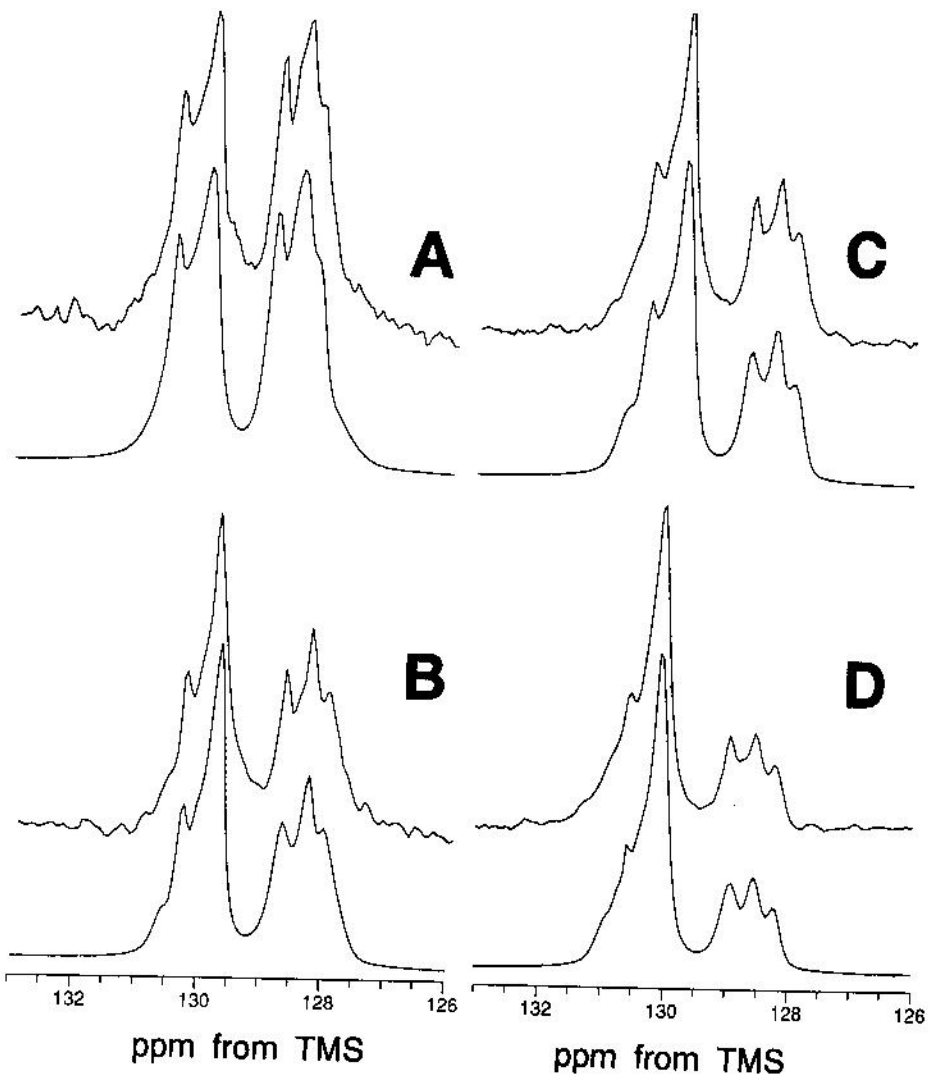

FIG. 6. 125.7 MHz (11.7 Tesla) ^{13}C MAS NMR spectra (top plot) and spectral simulations (bottom plot) of human myelin as a function of development, in the olefinic carbon region. (A) 4-month; (B) 15-month; (C) 48-month; (D) normal adult. The spectral simulations are based on coaddition of simulations of [18:1] and [20:4] diacyl-PC spectra (Fig. 7). The mole percentages of polyunsaturate were: (A) 36.8%; (B) 29.0%; (C) 18.6%; (D) 14.7%.

field from TMS for 4-month, 15-month, 48-month, and a normal adult human myelin. Based on the known fatty acid composition of myelin, and on the ^{13}C MAS NMR results for [18:1] and [20:4] fatty acyl chains, we can clearly see that there is a monotonic relative decrease in polyunsaturated fatty acids as a function of development, with the adult pattern being achieved at about 48 months, Fig. 6C and Fig. 7. This pattern of fatty acid development with age is wholly consistent with that reported previously (32), using conventional chromatographic techniques. It permits us to develop a "time-line" in which, either from a simple computer integration (*B/A* ratio) or from a more complex computer simulation, we can make a good estimate of the poly/monounsaturate ratio, as a function of developmental age, as shown in Fig. 7. The results of Figs. 6 and 7 thus indicate that the lipid hydrocarbon chains become more saturated as myelination proceeds—presumably resulting in an overall stabilization of the adult myelin membrane. Such a decrease in polyunsaturation would be expected to cause a decrease in lipid mobility as a function of developmental age, which may be amenable to, e.g., a ^{13}C CP-MAS NMR analysis, where in adult myelin we have already observed differential cross-relaxation rates (T_{CH}) for the monoenoic and polyenoic carbon atom sites (data not shown).

A demyelinating disease in which there are major changes in WM is the so-called Cree leukoencephalopathy (33), which is thought to arise from congenital demyelination, or defective myelin synthesis, much as seen in the murine mutants *jimpy*, *quaking*, *shiverer*, and *trembler*. Preliminary results of protein analysis indicated all expected protein components were present (M. Moscarello, to be published), but as seen in Fig. 8A, there are major differences between Cree leukoencephalopathy WM and a normal (15 month) infant myelin spectrum, Fig. 8B. Unfortunately, the spectral signal-to-noise ratio of the Cree WM spectrum is low—due to the fact that there is so little myelin. Clearly, there is very little GC present compared with normal myelin, the spectrum being, in fact, more similar to normal grey matter (25). Death occurs in 100% of reported cases within 21 months, consistent with the very poorly developed myelin.

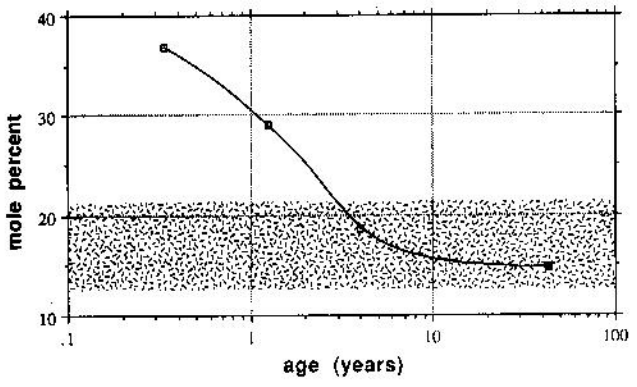

FIG. 7. Graph showing changes in polyunsaturated fatty acid content of human myelin as a function of development, experimental points from Fig. 6A–6D. The hatched region shows the mean (±1 SD, $n = 11$) for human adult myelin.

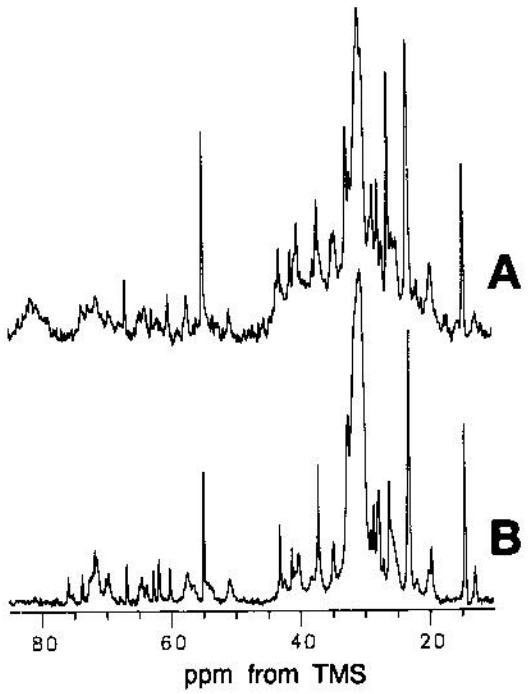

FIG. 8. 125.7 MHz (11.7 Tesla) proton-decoupled ^{13}C MAS NMR spectra of a Cree leukoencephalopathy white matter sample, together with a normal infant myelin. (A) Cree leukoencephalopathy white matter; (B) 15-month normal myelin.

Finally, we should note that we have obtained ^{13}C MAS NMR spectra of myelin from a range of other species, and find large differences in lipid compositional patterns (17). Work is now in progress to determine how such major compositional changes may (or may not) affect the dynamic structure (molecular motions) of myelin.

CONCLUSIONS

The results we have presented above are of interest for a number of reasons. First, we have been able to resolve a large number of resonances in the ^{13}C MAS NMR spectra of human (and bovine) WM and myelin, and have found no evidence for changes in spectral or sample appearance due to sample isolation, brain region, or to the relatively long periods required for data acquisition. Second, the majority of these features can be assigned—it is thus possible to identify, e.g., resonances due to GC-sugar residues, Cγ of PC/SM, cholesterol ring, and angular methyl carbons, arg-Cζ, [18:1/24:1] and [20:4] olefinic carbons, etc., as discussed in the text. Third, we have observed changes in myelin spectra as a function of myelin development, the major changes being due to a decrease in polyunsaturation with age. Fourth, preliminary observations on an abnormal infant Cree leukoencephalopathy WM indicated remarkable changes, due to poor myelination.

Overall, we believe these results show considerable promise for further work aimed at probing the interactions between the lipid/sterol and protein components in

myelin, since there are "marker" resonances for each of the major myelin lipid classes. Studies of lipid molecular motions may be particularly informative in understanding topics such as contrast enhancement in magnetic resonance imaging. If, as it appears, CHOL is involved in cross-relaxation with H_2O, then changes in CHOL correlation times—due, e.g., to changes in unsaturation or protein-lipid interaction—may affect image contrast (35, 36). In addition, the whole topic of cross-polarization in myelin, where T_{CH} values from <1 to >30 msec have been observed (as have oscillatory cross-polarization behaviors, Ref. 25), is likely to be of interest, given that most of the major lipid classes can now be separately identified, based on the assignments we have given above.

ACKNOWLEDGMENTS

We thank Brian Phillips for providing his spectral deconvolution/quantitation program (NMRFIT) to us and instructing us in its use; Amy Husted, Michaela Evangelista, and Matthew Hill for help with myelin preparations and data analysis; and Rick Olson of the Center for Electron Microscopy, University of Illinois, for his assistance with the electron microscopy. Some human brain samples were obtained from the National Neurological Research Bank, Veteran's Administration Medical Center, Wadsworth Division, Los Angeles, CA 90073, which is sponsored by NINDS/NIMH, National Multiple Sclerosis Society, Huntington's Disease Foundation, Comprehensive Epilepsy Program, Tourette Syndrome Association, Dystonia Medical Research Foundation, and Veterans Health Services and Research Administration, Department of Veterans Affairs.

REFERENCES

1. Z. Veksli, N. J. Salsbury, D. Chapman. *Biochim. Biophys. Acta* **183,** 434 (1969).
2. D. Chapman, S. A. Penkett. *Nature* **211,** 1304 (1966).
3. S. A. Penkett, A. G. Flook, D. Chapman. *Chem. Phys. Lipids* **2,** 273 (1968).
4. D. Chapman, D. J. Fluck, S. A. Penkett, G. G. Shipley. *Biochim. Biophys. Acta* **163,** 255 (1968).
5. E. Oldfield, D. Chapman, W. Derbyshire. *FEBS Lett.* **16,** 102 (1971).
6. R. L. Smith, E. Oldfield. *Science* **225,** 280 (1984).
7. D. Chapman, V. B. Kamat. *Regul. Funct. Biol. Membranes, Proc. Sigrid Jesulius Symp.* **2nd 11,** 99 (1968).
8. T. J. Jenkinson, V. B. Kamat, D. Chapman. *Biochim. Biophys. Acta.* **183,** 427 (1969).
9. E. C. Williams, E. H. Cordes. *Biochemistry* **15,** 5792 (1976).
10. Y. Wedmid, A. C. Lais, P. J. Dyck, W. J. Baumann. *Biochem. Biophys. Res. Commun.* **97,** 139 (1980).
11. E. Oldfield, J. L. Bowers, J. Forbes. *Biochemistry* **26,** 6919 (1987).
12. J. Forbes, J. Bowers, X. Shan, L. Moran, E. Oldfield, M. Moscarello. *J. Chem. Soc. Faraday Trans. I* **84,** 3821 (1988).
13. J. Forbes, C. Husted, E. Oldfield. *J. Am. Chem. Soc.* **110,** 1059 (1988).
14. J. R. Brainard, E. H. Cordes. *Biochemistry* **20,** 4607 (1981).
15. W. T. Norton, W. Cammer. *in* "Myelin" (P. Morell, Ed.), p. 155, Plenum Press, New York (1984).
16. P. S. Sastry. *Prog. Lipid. Res.* **24,** 69 (1985).
17. deleted in proof.
18. deleted in proof.
19. D. I. Hoult, R. E. Richards. *Proc. R. Soc. London, Ser. A.* **344,** 311 (1975).
20. J. C. Dittmer, R. L. Lester. *J. Lipid Res.* **5,** 126 (1964).
21. W. T. Norton. *Methods Enzymol.* **31,** 435 (1974).
22. U. K. Laemmli. *Nature* **227,** 680 (1970).
23. E. Oldfield, R. S. Norton, A. Allerhand. *J. Biol. Chem.* **250,** 6381 (1975).
24. M. B. Lees, S. W. Brostoff. *in* "Myelin" (P. Morell, Ed.), pp. 197–224, Plenum Press, New York (1984).
25. C. Husted, Ph.D. Thesis, University of Illinois at Urbana-Champaign (1990).
26. M. Bárány, C. Arus, Y.-C. Chang. *Magn. Res. Med.* **2,** 289 (1985).
27. D. C. Sheehan, B. B. Hrapchak. *in* "Theory and Practice of Histotechnology," pp. 261–262, Mosby, St. Louis (1980).
28. R. Murari, M. M. A. A. El-Rahman, Y. Wedmid, S. Parthasarathy, W. J. Baumann. *J. Org. Chem.* **47,** 2158 (1982).
29. J. G. Batchelor, R. J. Cushley, J. H. Prestegard. *J. Org. Chem.* **39,** 1698 (1974).
30. L. O. Sillerud, C. H. Han, M. W. Bitensky, A. A. Francendese. *J. Biol. Chem.* **261,** 4380 (1986).
31. L. Svennerholm, M. T. Vanier. *Brain Res.* **50,** 341 (1973).
32. L. Svennerholm, M. T. Vanier, B. Jungbjer. *J. Neurochem.* **30,** 1383 (1978).
33. D. N. Black, F. Booth, G. V. Watters, E. Andermann, C. Dumont, W. C. Halliday, J. Hoogstraten, M. E. Kabay, P. Kaplan, K. Meagher-Villemure, J. Michaud, G. O'Gorman. *Ann. Neurol.* **24,** 490 (1988).
34. deleted in proof.
35. S. H. Koenig, R. D. Brown, III, M. Spiller, N. Lundbom. *Mag. Res. Med.* **14,** 482 (1990).
36. T. A. Fralix, T. L. Ceckler, S. D. Wolff, S. A. Simon, R. S. Balaban. *Mag. Res. Med.* **18,** 214 (1991).
37. K. S. Bruzik. *J. Chem. Soc. Perkin Trans.* **I,** 423 (1988).
38. J. Dabrowski, H. Egge, P. Hanfland. *Chem. Phys. Lipids* **26,** 187 (1980).
39. T. Taketomi, A. Hara, Y. Kutsukake, E. Sugiyama. *J. Biochem.* **107,** 680 (1990).
40. A. C. McLaughlin. *Biochemistry* **21,** 4879 (1982).
41. E. Oldfield, F. Adebodun, J. Chung, B. Montez, K. D. Park, H. Le, B. Phillips. *Biochemistry* **30,** 11025 (1991).
42. J. C. Lindon, D. J. Baker, R. D. Farrant, J. M. Williams. *Biochem. J.* **233,** 275 (1986).
43. D. E. Dorman, S. J. Angyal, J. D. Roberts. *Proc. Natl. Acad. Sci.* **63,** 612 (1969).